

CERN-PH-EP-2013-100
16 June 2013

Directed flow of charged particles at mid-rapidity relative to the spectator plane in Pb–Pb collisions at $\sqrt{s_{NN}} = 2.76$ TeV

ALICE Collaboration*

Abstract

The directed flow of charged particles at mid-rapidity is measured in Pb–Pb collisions at $\sqrt{s_{NN}} = 2.76$ TeV relative to the collision symmetry plane defined by the spectator nucleons. A negative slope of the rapidity-odd directed flow component with approximately 3 times smaller magnitude than found at the highest RHIC energy is observed. This suggests a smaller longitudinal tilt of the initial system and disfavors the strong fireball rotation predicted for the LHC energies. The rapidity-even directed flow component is measured for the first time with spectators and found to be independent of pseudorapidity with a sign change at transverse momenta p_T between 1.2 and 1.7 GeV/ c . Combined with the observation of a vanishing rapidity-even p_T shift along the spectator deflection this is strong evidence for dipole-like initial density fluctuations in the overlap zone of the nuclei. Similar trends in the rapidity-even directed flow and the estimate from two-particle correlations at mid-rapidity, which is larger by about a factor of 40, indicate a weak correlation between fluctuating participant and spectator symmetry planes. These observations open new possibilities for investigation of the initial conditions in heavy-ion collisions with spectator nucleons.

arXiv:1306.4145v4 [nucl-ex] 2 Feb 2015

*See Appendix A for the list of collaboration members

The goal of the heavy-ion program at the Large Hadron Collider (LHC) is to explore the properties of deconfined quark-gluon matter. Anisotropic transverse flow is sensitive to the early times of the collision, when the deconfined state of quarks and gluons is expected to dominate the collision dynamics (see reviews [1, 2, 3] and references therein), with a positive (in-plane) elliptic flow as first observed at the Alternating Gradient Synchrotron (AGS) [4, 5]. A much stronger flow was subsequently measured at the Super Proton Synchrotron (SPS) [6], Relativistic Heavy Ion Collider (RHIC) [7, 8, 9] and recently at the LHC [10, 11, 12]. Elliptic flow at RHIC and the LHC is reproduced by hydrodynamic model calculations with a small value of the ratio of shear viscosity to entropy density [13, 14, 15, 16]. Despite the success of hydrodynamics in describing the equilibrium phase of matter produced in a relativistic heavy-ion collision, there are still large theoretical uncertainties in determination of the initial conditions. Significant triangular flow measured recently at RHIC [17, 18] and LHC [19, 20, 12] energies has demonstrated [21, 22] that initial energy fluctuations play an important role in the development of the final momentum-space anisotropy of the distribution of produced particles.

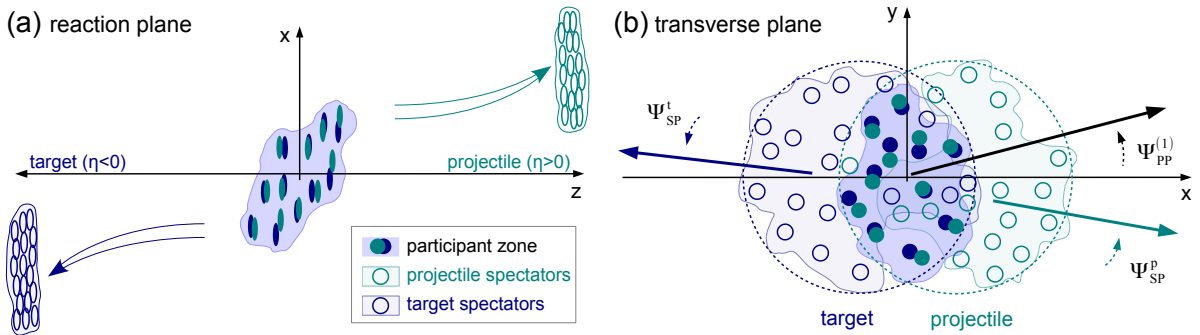


Fig. 1: (color online) Sketch of a non-central heavy-ion collision. See text for description of the figure.

The collision geometry is illustrated in Fig. 1 which depicts the participant overlap region and spectators as viewed in (a) the reaction plane and (b) the plane perpendicular to the beam. Figure 1(a) shows the projectile and target spectators repelled in the reaction (xz) plane from the center of the colliding system along the impact parameter (x) direction. An alternative scenario where spectators are attracted towards the center of the system is discussed in [23].

The directed flow is characterized by the first harmonic coefficient v_1 in a Fourier decomposition of the particle azimuthal distribution with respect to one of the collision symmetry planes, Ψ , as illustrated in Fig. 1(b) and discussed below

$$v_1(\eta, p_T)\{\Psi\} = \langle \cos(\phi - \Psi) \rangle. \quad (1)$$

Here $\eta = -\ln[\tan(\theta/2)]$, p_T , θ and ϕ are the particle pseudorapidity, transverse momentum, polar and azimuthal angles, respectively. The brackets " $\langle \dots \rangle$ " indicate an average over measured particles in all recorded events.

For a non-fluctuating nuclear matter distribution, the directed flow in the participant zone develops along the impact parameter direction. The collision symmetry requires that the directed flow be an anti-symmetric function of pseudorapidity, $v_1^{\text{odd}}(\eta) = -v_1^{\text{odd}}(-\eta)$. Due to event-by-event fluctuations in the initial energy density of the collision, the participant plane angle ($\Psi_{\text{PP}}^{(1)}$) defined by the dipole asymmetry of the initial energy density [24, 25] and that of projectile ($\Psi_{\text{SP}}^{\text{p}}$) and target ($\Psi_{\text{SP}}^{\text{t}}$) spectators are different from the geometrical reaction plane angle Ψ_{RP} (x -axis in Fig. 1(b)). As a consequence, the directed flow can develop [24, 25, 26, 27] a rapidity-symmetric component, $v_1^{\text{even}}(\eta) = v_1^{\text{even}}(-\eta)$, which does not vanish at mid-rapidity.

The slope of v_1^{odd} as a function of rapidity at AGS [5, 28] and SPS [29, 30] energies is driven by the difference between baryon and meson production and shadowing by the nuclear remnants. At higher

(RHIC) energies a multiple zero crossing of v_1^{odd} with rapidity outside the nuclear fragmentation regions was predicted as a signature of the deconfined phase transition [31, 32]. However, the RHIC measurements [33, 34, 35, 36] did not reveal such a structure. The magnitude of the directed flow depends on the amount of baryon stopping in the nuclear overlap zone [37]. The two can be related via realistic model calculations, making v_1^{odd} an important experimental probe of the initial conditions in a heavy-ion collision. The initial conditions assumed in model calculations of v_1^{odd} range from incomplete baryon stopping [37], with a positive space-momentum correlation, to full nucleon stopping with a tilted [32, 38] or rotating [39] source of matter produced in the overlap zone of the nuclei. Model calculations generally agree on the negative sign of the v_1^{odd} slope as a function of pseudorapidity at RHIC [33, 34, 35, 36]. The model predictions for v_1^{odd} at the LHC vary from having the same slope as at RHIC but with smaller magnitude [38] to an opposite (positive) slope with significantly larger magnitude [40, 39].

The v_1^{even} estimated from the two-particle azimuthal correlations at mid-rapidity for RHIC [41] (see also [25]) and LHC [42, 12, 20] energies is in approximate agreement with ideal hydrodynamic model calculations [26, 27] for dipole-like [24] energy fluctuations in the overlap zone of the nuclei. Interpretation of the two-particle correlations is complicated due to a possibly large bias from correlations unrelated to the initial geometry (non-flow) and due to the model dependence of the correction procedure for effects of momentum conservation [27]. The directed flow measured relative to the spectator deflection is free from such biases and provides a cleaner probe of the initial conditions in a heavy-ion collision. It also allows for a study of the main features of the dipole-like energy fluctuations such as a vanishing transverse momentum shift of the created system along the direction of the spectator deflection. Directed flow and its fluctuations also play an important role in understanding effects due to the strong magnetic field in heavy-ion collisions [24] and interpretation of the observed charge separation relative to the reaction plane [43] in terms of the chiral magnetic effect [44].

In this Letter, we report the charged particle directed flow measured relative to the deflection of spectator neutrons in Pb–Pb collisions at $\sqrt{s_{\text{NN}}} = 2.76$ TeV. About 13 million minimum-bias [10] collisions in the 5-80% centrality range were analyzed. For the most central (0-5%) collisions, the small number of spectators does not allow for a reliable reconstruction of their deflection. Two forward scintillator arrays (VZERO) [45] were used to determine the collision centrality. Charged particles reconstructed in the Time Projection Chamber (TPC) [46] with $p_{\text{T}} > 0.15$ GeV/c and $|\eta| < 0.8$ were selected for the analysis.

The deflection of neutron spectators was reconstructed using a pair of Zero Degree Calorimeters (ZDC) [47] with 2×2 segmentation installed 114 meters from the interaction point on each side, covering the $|\eta| > 8.78$ (beam rapidity) region. A typical energy measured by both ZDCs for 30-40% centrality is about 100 TeV [48]. The spectator deflection in the transverse plane was measured with a pair of two-dimensional vectors

$$\mathbf{Q}^{\text{t,p}} \equiv (\mathbf{Q}_x^{\text{t,p}}, \mathbf{Q}_y^{\text{t,p}}) = \frac{\sum_{i=1}^4 \mathbf{n}_i E_i^{\text{t,p}}}{\sum_{i=1}^4 E_i^{\text{t,p}}}, \quad (2)$$

where \mathbf{p} (t) denotes the ZDC on the $\eta > 0$ ($\eta < 0$) side of the interaction point, E_i is the measured signal and $\mathbf{n}_i = (x_i, y_i)$ are the coordinates of the i -th ZDC segment. An asymmetry of 0.1% [49] in energy calibration of the two ZDCs and an absolute energy scale uncertainty cancel in Eq. (2). To compensate for the run-dependent variation of the LHC beam crossing position, an event-by-event correction $\mathbf{Q}^{\text{t,p}} \rightarrow \mathbf{Q}^{\text{t,p}} - \langle \mathbf{Q}^{\text{t,p}} \rangle$ [3] was applied as a function of collision centrality and transverse position of the collision vertex relative to the center of the ALICE detector. Experimental values of the correction for the 30-40% centrality class are $\langle \mathbf{Q}_{x(y)}^{\text{p}} \rangle \approx 2.0$ (−1.5) mm and $\langle \mathbf{Q}_{x(y)}^{\text{t}} \rangle \approx -1.1$ (0.01) mm.

The directed flow is determined with the scalar product method [3, 50]

$$\begin{aligned} v_1\{\Psi_{\text{SP}}^{\text{p}}\} &= \frac{1}{\sqrt{2}} \left[\frac{\langle u_x Q_x^{\text{p}} \rangle}{\sqrt{|\langle Q_x^{\text{t}} Q_x^{\text{p}} \rangle|}} + \frac{\langle u_y Q_y^{\text{p}} \rangle}{\sqrt{|\langle Q_y^{\text{t}} Q_y^{\text{p}} \rangle|}} \right], \\ v_1\{\Psi_{\text{SP}}^{\text{t}}\} &= -\frac{1}{\sqrt{2}} \left[\frac{\langle u_x Q_x^{\text{t}} \rangle}{\sqrt{|\langle Q_x^{\text{t}} Q_x^{\text{p}} \rangle|}} + \frac{\langle u_y Q_y^{\text{t}} \rangle}{\sqrt{|\langle Q_y^{\text{t}} Q_y^{\text{p}} \rangle|}} \right] \end{aligned} \quad (3)$$

where $u_x = \cos\phi$ and $u_y = \sin\phi$ are defined for charged particles at midrapidity. The odd and even components of the directed flow relative to the spectator plane ($\Psi = \Psi_{\text{SP}}$ in Eq. (1)) are then calculated from the equations

$$v_1^{\text{odd}}\{\Psi_{\text{SP}}\} = [v_1\{\Psi_{\text{SP}}^{\text{p}}\} + v_1\{\Psi_{\text{SP}}^{\text{t}}\}]/2 \quad (4)$$

and

$$v_1^{\text{even}}\{\Psi_{\text{SP}}\} = [v_1\{\Psi_{\text{SP}}^{\text{p}}\} - v_1\{\Psi_{\text{SP}}^{\text{t}}\}]/2. \quad (5)$$

Equation (4) defines the sign of v_1^{odd} using the convention used at RHIC [33, 34] and implies a positive directed flow (or deflection along the positive x -axis direction in Fig. 1(a)) of the projectile spectators.

The negative correlations $\langle Q_x^{\text{t}} Q_x^{\text{p}} \rangle$ and $\langle Q_y^{\text{t}} Q_y^{\text{p}} \rangle$ [51] indicate a deflection of the projectile and target spectators in opposite directions. These correlations are sensitive to a combination of the spectator's directed flow relative to the reaction plane Ψ_{RP} and an additional contribution due to flow of spectators along the fluctuating $\Psi_{\text{SP}}^{\text{p}}$ and $\Psi_{\text{SP}}^{\text{t}}$ directions (see Fig. 1(b)). The two contributions are not separable using current experimental techniques and both should be considered in theoretical interpretations of the results derived from Eqs. (3)-(5). Given that the transverse deflection of spectators ($d_{\text{spec}} \approx \sqrt{(\langle Q_x^{\text{t}} Q_x^{\text{p}} \rangle + \langle Q_y^{\text{t}} Q_y^{\text{p}} \rangle) / 2}$) is tiny compared to the ZDC detector position $|z_{\text{ZDC}}| = 114$ m along the beam direction, one can make a rough estimate of the corresponding transverse momentum carried by an individual spectator: $p_{\text{T}}^{\text{spec}} \approx \sqrt{s_{\text{NN}}} (d_{\text{spec}} / z_{\text{ZDC}})$. The measured d_{spec} is about 0.67 (0.92) mm [51] for the 5-10% (30-40%) centrality class which yields $p_{\text{T}}^{\text{spec}} \sim 16$ (22) MeV/ c . Correlations $\langle Q_x^{\text{t}} Q_y^{\text{p}} \rangle$ and $\langle Q_y^{\text{t}} Q_x^{\text{p}} \rangle$ in orthogonal directions, which can be non-zero due to residual detector effects, are less than 5% [51] of those in the aligned directions. The 10-20% [51] difference between $\langle Q_x^{\text{t}} Q_x^{\text{p}} \rangle$ and $\langle Q_y^{\text{t}} Q_y^{\text{p}} \rangle$ for mid-central collisions is mainly due to a different offset of the beam spot from the center of the ZDCs in-plane and perpendicular to the LHC accelerator ring. The corresponding dominant systematic uncertainty is evaluated from the spread of results for different terms in Eq. (3) and estimated to be below 20%. The results obtained with Eq. (3) are consistent with calculations using the event plane method [3]. The results with opposite polarity of the magnetic field of the ALICE detector are consistent within 5%. Variation of the results with the collision centrality estimated with the TPC, VZERO, and Silicon Pixel Detectors [47] and with narrowing the nominal ± 10 cm range of the collision vertex along the beam direction from the center of the ALICE detector to ± 7 cm is less than 5%. Altering the selection criteria for the tracks reconstructed with the TPC resulted in a 3-5% variation of the results. The systematic error evaluated for each of the sources listed above were added in quadrature to obtain the total systematic uncertainty of the measurement.

Figure 2(a) shows the charged particle directed flow as a function of pseudorapidity for 10-20%, 30-40%, and 10-60% centrality classes. The $v_1^{\text{even}}(\eta)$ component is found to be negative and independent of η . The $v_1^{\text{odd}}(\eta)$ component exhibits a negative slope as a function of pseudorapidity. This is in contrast to the positive slope expected from the model calculations [40, 39] with stronger rotation of the participant zone at the LHC than at RHIC. The $v_1^{\text{odd}}(\eta)$ at the highest RHIC energy [34] has the same sign of the slope and a factor of three larger magnitude. This is consistent with a smaller tilt of the participant zone in the x - z plane (see Fig. 1(a)) as predicted in [38] for LHC energies. Figure 2(c) compares v_1^{odd} with the STAR data [34] for Au-Au collisions at $\sqrt{s_{\text{NN}}} = 200$ (62) GeV downscaled by the ratio 0.37 (0.12) of the slope at the LHC to that at RHIC energy. These ratios indicate a strong violation by a factor of 1.82 (4.55) of the beam rapidity scaling discussed in [36].

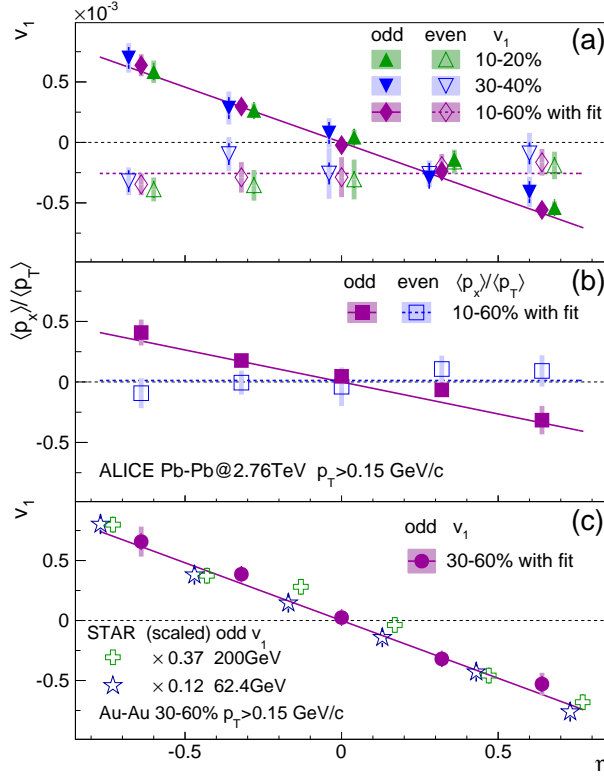


Fig. 2: (color online) (a) v_1 and (b) $\langle p_x \rangle / \langle p_T \rangle$ versus pseudorapidity in Pb–Pb collisions at $\sqrt{s_{NN}} = 2.76$ TeV. (c) v_1^{odd} compared to the STAR data [34] for Au–Au collisions at $\sqrt{s_{NN}} = 200$ (62.4) GeV downscaled by a factor 0.37 (0.12). The statistical (systematic) uncertainties are indicated by the error bars (shaded bands). Lines (to guide the eye) represent fits with a linear (constant) function for v_1^{odd} (v_1^{even}).

Figure 2(b) shows the relative momentum shift $\langle p_x \rangle / \langle p_T \rangle \equiv \langle p_T \cos(\phi - \Psi_{SP}) \rangle / \langle p_T \rangle$, along the spectator plane as a function of pseudorapidity. It is obtained by introducing a $p_T / \langle p_T \rangle$ weight in front of u_x and u_y in Eq. (3). The non-zero $\langle p_x \rangle^{\text{odd}} / \langle p_T \rangle$ shift has a smaller magnitude than v_1^{odd} . The $\langle p_x \rangle^{\text{even}}$ vanishes which is consistent with the dipole-like event-by-event fluctuations of the initial energy density in a system with zero net transverse momentum. Disappearance of $\langle p_x \rangle$ at $\eta \approx 0$ indicates that particles produced at mid-rapidity are not involved in balancing the transverse momentum carried away by spectators.

Figures 3(a) and 3(b) present v_1 and $\langle p_x \rangle / \langle p_T \rangle$ versus collision centrality. The odd components were calculated by taking values at negative η with an opposite sign. Both v_1 components have weak centrality dependence. The $\langle p_x \rangle^{\text{even}}$ component is zero at all centralities, while $\langle p_x \rangle^{\text{odd}} / \langle p_T \rangle$ is a steeper function of centrality than v_1^{odd} . This suggests that v_1^{odd} has two contributions. The first contribution has a similar origin as v_1^{even} due to asymmetric dipole-like initial energy fluctuations. The second contribution grows almost linearly from central to peripheral collisions and represents an effect of sideward collective motion of particles at non-zero rapidity due to expansion of the initially tilted source. This $\langle p_x \rangle$ is balanced by that of the particles produced at opposite rapidity and in very forward (spectator) regions. The magnitude of v_1^{odd} at the LHC is significantly smaller than at RHIC with a similar centrality dependence (see Fig. 3(c)).

Figure 4(a) presents v_1 as a function of p_T . Both components change sign around p_T between 1.2 – 1.7 GeV/c which is expected for the dipole-like energy fluctuations when the momentum of the low p_T particles is balanced by those at high p_T [24, 25, 26, 27]. The p_T dependence of v_1^{even} relative to Ψ_{SP} is similar to that of v_1^{even} relative to $\Psi_{pp}^{(1)}$ estimated from the Fourier fits of the two-particle correlations [42, 12, 20],

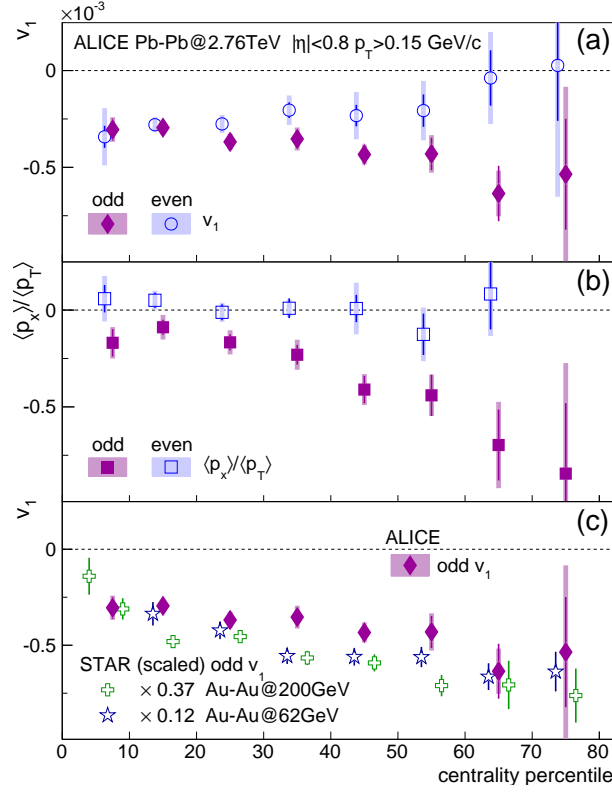


Fig. 3: (color online) (a) v_1 and (b) $\langle p_x \rangle / \langle p_T \rangle$ versus centrality. (c) v_1^{odd} comparison with STAR data [34]. See text and Fig. 2 for description of the data points.

while its magnitude is smaller by a factor of forty [27, 52]. This can be interpreted as a weak correlation, $\langle \cos(\Psi_{\text{PP}}^{(1)} - \Psi_{\text{SP}}) \rangle \ll 1$, between the orientation of the participant and spectator collision symmetry planes. Compared to the RHIC measurements in Fig. 4(b), v_1^{odd} shows a similar trend including the sign change around p_T of 1.5 GeV/c in central collisions and a negative value at all p_T for peripheral collisions.

According to hydrodynamic model calculations [53, 24, 27] particles with low p_T should flow in the direction opposite to the largest density gradient. This, together with the negative even and odd v_1 components relative to Ψ_{SP} measured for particles at mid-rapidity with low transverse momentum ($p_T \lesssim 1.2$ GeV/c) allows to determine if spectators deflect away from or towards the center of the system. However, a detailed theoretical calculation of the correlation between fluctuations in the spectator positions and energy density in the participant zone such as in [23] is required to provide a definitive answer to this question.

In summary, the v_1^{odd} and v_1^{even} components of charged particle directed flow at mid-rapidity, $|\eta| < 0.8$, are measured relative to the spectator plane for Pb–Pb collisions at $\sqrt{s_{\text{NN}}} = 2.76$ TeV. The v_1^{odd} has a negative slope as a function of pseudorapidity with a magnitude about three times smaller than at the highest RHIC energy. This suggests a smaller tilt of the medium created in the participant zone at the LHC, with insufficient rotation to alter the slope of $v_1^{\text{odd}}(\eta)$ as predicted in [40, 39]. As a function of p_T , v_1^{odd} and v_1^{even} cross zero at p_T between 1.2 – 1.7 GeV/c for semi-central collisions. Disappearance of $\langle p_x \rangle$ for particles produced close to zero rapidity suggest that they do not play a role in balancing the p_T kick of spectators. The shape of $v_1^{\text{even}}(p_T)$ and a vanishing $\langle p_x \rangle^{\text{even}}$ is consistent with dipole-like fluctuations of the initial energy density in the participant zone. A similar shape but with about forty times larger magnitude was observed for an estimate of $v_1^{\text{even}}(p_T)$ relative to the participant plane from the Fourier fits of the two-particle correlation [42, 12]. This indicates that fluctuating participant and

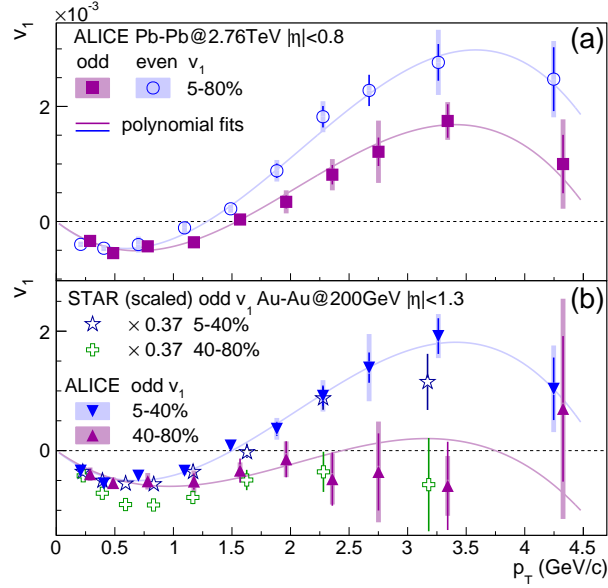


Fig. 4: (color online) (a) v_1 versus transverse momentum. (b) v_1^{odd} comparison with STAR data [34]. See text and Fig. 2 for description of the data points. Lines (to guide the eye) represent fits with a third order polynomial.

spectator collision symmetry planes are weakly correlated, which is important experimental input for modeling the ill-constrained initial conditions of a heavy-ion collision. Future studies of the directed flow at mid-rapidity using identified particles and extension of the v_1 measurements to forward rapidities should provide a stronger constraint on the effects of initial density fluctuations in the formation of directed flow.

Acknowledgements

The ALICE collaboration would like to thank all its engineers and technicians for their invaluable contributions to the construction of the experiment and the CERN accelerator teams for the outstanding performance of the LHC complex. The ALICE collaboration acknowledges the following funding agencies for their support in building and running the ALICE detector: State Committee of Science, World Federation of Scientists (WFS) and Swiss Fonds Kidagan, Armenia, Conselho Nacional de Desenvolvimento Científico e Tecnológico (CNPq), Financiadora de Estudos e Projetos (FINEP), Fundação de Amparo à Pesquisa do Estado de São Paulo (FAPESP); National Natural Science Foundation of China (NSFC), the Chinese Ministry of Education (CMOE) and the Ministry of Science and Technology of China (MSTC); Ministry of Education and Youth of the Czech Republic; Danish Natural Science Research Council, the Carlsberg Foundation and the Danish National Research Foundation; The European Research Council under the European Community's Seventh Framework Programme; Helsinki Institute of Physics and the Academy of Finland; French CNRS-IN2P3, the 'Region Pays de Loire', 'Region Alsace', 'Region Auvergne' and CEA, France; German BMBF and the Helmholtz Association; General Secretariat for Research and Technology, Ministry of Development, Greece; Hungarian OTKA and National Office for Research and Technology (NKTH); Department of Atomic Energy and Department of Science and Technology of the Government of India; Istituto Nazionale di Fisica Nucleare (INFN) and Centro Fermi - Museo Storico della Fisica e Centro Studi e Ricerche "Enrico Fermi", Italy; MEXT Grant-in-Aid for Specially Promoted Research, Japan; Joint Institute for Nuclear Research, Dubna; National Research Foundation of Korea (NRF); CONACYT, DGAPA, México, ALFA-EC and the EPLANET Program (European Particle Physics Latin American Network) Stichting voor Fundamenteel Onderzoek der Materie (FOM) and the Nederlandse Organisatie voor Wetenschappelijk Onderzoek (NWO), Netherlands; Re-

search Council of Norway (NFR); Polish Ministry of Science and Higher Education; National Authority for Scientific Research - NASR (Autoritatea Națională pentru Cercetare Științifică - ANCS); Ministry of Education and Science of Russian Federation, Russian Academy of Sciences, Russian Federal Agency of Atomic Energy, Russian Federal Agency for Science and Innovations and The Russian Foundation for Basic Research; Ministry of Education of Slovakia; Department of Science and Technology, South Africa; CIEMAT, EELA, Ministerio de Economía y Competitividad (MINECO) of Spain, Xunta de Galicia (Consellería de Educación), CEADEN, Cubaenergía, Cuba, and IAEA (International Atomic Energy Agency); Swedish Research Council (VR) and Knut & Alice Wallenberg Foundation (KAW); Ukraine Ministry of Education and Science; United Kingdom Science and Technology Facilities Council (STFC); The United States Department of Energy, the United States National Science Foundation, the State of Texas, and the State of Ohio.

References

- [1] W. Reisdorf and H. Ritter, *Collective flow in heavy-ion collisions*, *Ann. Rev. Nucl. Part. Sci.* **47**, 663 (1997), doi:10.1146/annurev.nucl.47.1.663.
- [2] N. Herrmann, J. Wessels and T. Wienold, *Collective flow in heavy ion collisions*, *Ann. Rev. Nucl. Part. Sci.* **49**, 581 (1999), doi:10.1146/annurev.nucl.49.1.581.
- [3] S. A. Voloshin, A. M. Poskanzer and R. Snellings, *Collective phenomena in non-central nuclear collisions*, in Landolt-Boernstein, *Relativistic Heavy Ion Physics*, Vol. **1/23**, 5 (Springer-Verlag, 2010).
- [4] E877 Collaboration, J. Barrette *et al.*, *Observation of anisotropic event shapes and transverse flow in Au + Au collisions at AGS energy*, *Phys. Rev. Lett.* **73**, 2532 (1994), doi:10.1103/PhysRevLett.73.2532.
- [5] E877 Collaboration, J. Barrette *et al.*, *Energy and charged particle flow in a 10.8-A/GeV/c Au + Au collisions*, *Phys. Rev.* **C55**, 1420 (1997), doi:10.1103/PhysRevC.55.1420, 10.1103/PhysRevC.56.2336.
- [6] NA49 Collaboration, H. Appelshauser *et al.*, *Directed and elliptic flow in 158-GeV/nucleon Pb + Pb collisions*, *Phys. Rev. Lett.* **80**, 4136 (1998), doi:10.1103/PhysRevLett.80.4136.
- [7] STAR Collaboration, K. Ackermann *et al.*, *Elliptic flow in Au + Au collisions at $\sqrt{s_{NN}} = 130$ GeV*, *Phys. Rev. Lett.* **86**, 402 (2001).
- [8] PHENIX Collaboration, K. Adcox *et al.*, *Flow measurements via two particle azimuthal correlations in Au+Au collisions at $\sqrt{s_{NN}} = 130$ -GeV*, *Phys. Rev. Lett.* **89**, 212301 (2002).
- [9] PHOBOS Collaboration, B. Back *et al.*, *Energy dependence of elliptic flow over a large pseudorapidity range in Au+Au collisions at RHIC*, *Phys. Rev. Lett.* **94**, 122303 (2005), doi:10.1103/PhysRevLett.94.122303.
- [10] ALICE Collaboration, K. Aamodt *et al.*, *Elliptic flow of charged particles in Pb–Pb collisions at 2.76 TeV*, *Phys. Rev. Lett.* **105**, 252302 (2010), doi:10.1103/PhysRevLett.105.252302.
- [11] CMS Collaboration, S. Chatrchyan *et al.*, *Measurement of the elliptic anisotropy of charged particles produced in Pb–Pb collisions at nucleon-nucleon center-of-mass energy = 2.76 TeV*, *Phys. Rev.* **C87**, 014902 (2013), doi:10.1103/PhysRevC.87.014902.
- [12] ATLAS Collaboration, G. Aad *et al.*, *Measurement of the azimuthal anisotropy for charged particle production in $\sqrt{s_{NN}} = 2.76$ TeV lead-lead collisions with the ATLAS detector*, *Phys. Rev.* **C86**, 014907 (2012), doi:10.1103/PhysRevC.86.014907.
- [13] P. Huovinen, P. Kolb, U. W. Heinz, P. Ruuskanen and S. Voloshin, *Radial and elliptic flow at RHIC: Further predictions*, *Phys. Lett.* **B503**, 58 (2001), doi:10.1016/S0370-2693(01)00219-2.
- [14] U. W. Heinz, C. Shen and H. Song, *The viscosity of quark-gluon plasma at RHIC and the LHC*, *AIP Conf.Proc.* **1441**, 766 (2012).

- [15] H. Song and U. W. Heinz, *Suppression of elliptic flow in a minimally viscous quark-gluon plasma*, Phys. Lett. **B658**, 279 (2008), doi:10.1016/j.physletb.2007.11.019.
- [16] H. Song and U. W. Heinz, *Causal viscous hydrodynamics in 2+1 dimensions for relativistic heavy-ion collisions*, Phys. Rev. **C77**, 064901 (2008), doi:10.1103/PhysRevC.77.064901.
- [17] STAR Collaboration, L. Adamczyk *et al.*, *Third Harmonic Flow of Charged Particles in Au+Au Collisions at $\sqrt{s_{NN}} = 200$ GeV*, Phys. Rev. **C88**, 014904 (2013), doi:10.1103/PhysRevC.88.014904.
- [18] PHENIX Collaboration, A. Adare *et al.*, *Measurements of Higher-Order Flow Harmonics in Au+Au Collisions at $\sqrt{s_{NN}} = 200$ GeV*, Phys. Rev. Lett. **107**, 252301 (2011), doi:10.1103/PhysRevLett.107.252301.
- [19] ALICE Collaboration, K. Aamodt *et al.*, *Higher harmonic anisotropic flow measurements of charged particles in Pb–Pb collisions at $\sqrt{s_{NN}} = 2.76$ TeV*, Phys. Rev. Lett. **107**, 032301 (2011).
- [20] CMS Collaboration, S. Chatrchyan *et al.*, *Centrality dependence of dihadron correlations and azimuthal anisotropy harmonics in Pb–Pb collisions at $\sqrt{s_{NN}} = 2.76$ TeV*, Eur. Phys. J. **C72**, 2012 (2012), doi:10.1140/epjc/s10052-012-2012-3.
- [21] B. Alver and G. Roland, *Collision geometry fluctuations and triangular flow in heavy-ion collisions*, Phys. Rev. **C81**, 054905 (2010), doi:10.1103/PhysRevC.82.039903, 10.1103/PhysRevC.81.054905.
- [22] P. Sorensen, *Implications of space-momentum correlations and geometric fluctuations in heavy-ion collisions*, J. Phys. **G37**, 094011 (2010), doi:10.1088/0954-3899/37/9/094011.
- [23] M. Alvioli and M. Strikman, *Beam Fragmentation in Heavy Ion Collisions with Realistically Correlated Nuclear Configurations*, Phys. Rev. **C83**, 044905 (2011), doi:10.1103/PhysRevC.83.044905.
- [24] D. Teaney and L. Yan, *Triangularity and Dipole Asymmetry in Heavy Ion Collisions*, Phys. Rev. **C83**, 064904 (2011), doi:10.1103/PhysRevC.83.064904.
- [25] M. Luzum and J.-Y. Ollitrault, *Directed flow at midrapidity in heavy-ion collisions*, Phys. Rev. Lett. **106**, 102301 (2011), doi:10.1103/PhysRevLett.106.102301.
- [26] F. G. Gardim, F. Grassi, Y. Hama, M. Luzum and J.-Y. Ollitrault, *Directed flow at mid-rapidity in event-by-event hydrodynamics*, Phys. Rev. **C83**, 064901 (2011), doi:10.1103/PhysRevC.83.064901.
- [27] E. Retinskaya, M. Luzum and J.-Y. Ollitrault, *Directed flow at midrapidity in $\sqrt{s_{NN}} = 2.76$ TeV Pb+Pb collisions*, Phys. Rev. Lett. **108**, 252302 (2012), doi:10.1103/PhysRevLett.108.252302.
- [28] E877 Collaboration, J. Barrette *et al.*, *Proton and pion production relative to the reaction plane in Au + Au collisions at AGS energies*, Phys. Rev. **C56**, 3254 (1997), doi:10.1103/PhysRevC.56.3254.
- [29] NA49 Collaboration, C. Alt *et al.*, *Directed and elliptic flow of charged pions and protons in Pb + Pb collisions at 40-A-GeV and 158-A-GeV*, Phys. Rev. **C68**, 034903 (2003), doi:10.1103/PhysRevC.68.034903.
- [30] WA98 Collaboration, M. Aggarwal *et al.*, *Directed flow in 158-A-GeV Pb-208 + Pb-208 collisions*, nucl-ex/9807004, arXiv:nucl-ex/9807004.
- [31] J. Brachmann *et al.*, *Antiflow of nucleons at the softest point of the EoS*, Phys. Rev. **C61**, 024909 (2000), doi:10.1103/PhysRevC.61.024909.
- [32] L. Csernai and D. Röhrich, *Third flow component as QGP signal*, Phys. Lett. **B458**, 454 (1999), doi:10.1016/S0370-2693(99)00615-2.
- [33] STAR Collaboration, J. Adams *et al.*, *Directed flow in Au+Au collisions at $\sqrt{s_{NN}} = 62$ GeV*, Phys. Rev. **C73**, 034903 (2006), doi:10.1103/PhysRevC.73.034903.

- [34] STAR Collaboration, B. Abelev *et al.*, *System-size independence of directed flow at the Relativistic Heavy-Ion Collider*, Phys. Rev. Lett. **101**, 252301 (2008), doi:10.1103/PhysRevLett.101.252301.
- [35] PHOBOS Collaboration, B. Back *et al.*, *Energy dependence of directed flow over a wide range of pseudorapidity in Au + Au collisions at RHIC*, Phys. Rev. Lett. **97**, 012301 (2006), doi:10.1103/PhysRevLett.97.012301.
- [36] STAR Collaboration, G. Agakishiev *et al.*, *Directed and elliptic flow of charged particles in Cu+Cu collisions at $\sqrt{s_{NN}} = 22.4$ GeV*, Phys. Rev. **C85**, 014901 (2012), doi:10.1103/PhysRevC.85.014901.
- [37] R. Snellings, H. Sorge, S. Voloshin, F. Wang and N. Xu, *Novel rapidity dependence of directed flow in high-energy heavy ion collisions*, Phys. Rev. Lett. **84**, 2803 (2000), doi:10.1103/PhysRevLett.84.2803.
- [38] P. Bozek and I. Wyskiel, *Directed flow in ultrarelativistic heavy-ion collisions*, Phys. Rev. **C81**, 054902 (2010), doi:10.1103/PhysRevC.81.054902.
- [39] L. Csernai, V. Magas, H. Stöcker and D. Strottman, *Fluid Dynamical Prediction of Changed v_1 -flow at LHC*, Phys. Rev. **C84**, 024914 (2011), doi:10.1103/PhysRevC.84.024914.
- [40] J. Bleibel, G. Baur and C. Fuchs, *Anisotropic flow in Pb+Pb collisions at LHC from the quark gluon string model with parton rearrangement*, Phys. Lett. **B659**, 520 (2008), doi:10.1016/j.physletb.2007.11.042.
- [41] STAR Collaboration, H. Agakishiev *et al.*, *Measurements of Dihadron Correlations Relative to the Event Plane in Au+Au Collisions at $\sqrt{s_{NN}} = 200$ GeV*, 1010.0690, arXiv:1010.0690.
- [42] ALICE Collaboration, K. Aamodt *et al.*, *Harmonic decomposition of two-particle angular correlations in Pb–Pb collisions at $\sqrt{s_{NN}} = 2.76$ TeV*, Phys. Lett. **B708**, 249 (2012), doi:10.1016/j.physletb.2012.01.060.
- [43] ALICE Collaboration, B. Abelev *et al.*, *Charge separation relative to the reaction plane in Pb–Pb collisions at $\sqrt{s_{NN}} = 2.76$ TeV*, Phys. Rev. Lett. **110**, 012301 (2013).
- [44] K. Fukushima, D. E. Kharzeev and H. J. Warringa, *The Chiral Magnetic Effect*, Phys. Rev. **D78**, 074033 (2008), doi:10.1103/PhysRevD.78.074033.
- [45] ALICE Collaboration, K. Aamodt *et al.*, *The ALICE experiment at the CERN LHC*, JINST **3**, S08002 (2008).
- [46] J. Alme *et al.*, *The ALICE TPC, a large 3-dimensional tracking device with fast readout for ultra-high multiplicity events*, Nucl.Instrum.Meth. **A622**, 316 (2010), doi:10.1016/j.nima.2010.04.042.
- [47] ALICE Collaboration, F. Carminati *et al.*, *ALICE: Physics performance report, volume I*, J. Phys. **G30**, 1517 (2004).
- [48] ALICE Collaboration, B. Abelev *et al.*, *Centrality determination of Pb-Pb collisions at $\sqrt{s_{NN}} = 2.76$ TeV with ALICE*, 1301.4361, arXiv:1301.4361.
- [49] ALICE Collaboration, B. Abelev *et al.*, *Measurement of the Cross Section for Electromagnetic Dissociation with Neutron Emission in Pb-Pb Collisions at $\sqrt{s_{NN}} = 2.76$ TeV*, Phys. Rev. Lett. **109**, 252302 (2012), doi:10.1103/PhysRevLett.109.252302.
- [50] I. Selyuzhenkov and S. Voloshin, *Effects of non-uniform acceptance in anisotropic flow measurement*, Phys. Rev. **C77**, 034904 (2008), doi:10.1103/PhysRevC.77.034904.
- [51] ALICE Collaboration, B. Abelev *et al.*, *Results for $\langle Q_{x(y)}^p Q_{x(y)}^t \rangle$ and $\langle Q_{x(y)}^p Q_{y(x)}^t \rangle$ correlations*, <http://hepdata.cedar.ac.uk/view/ins1238980> (2013).
- [52] ALICE Collaboration, I. Selyuzhenkov, *Charged particle directed flow in Pb–Pb collisions at $\sqrt{s_{NN}} = 2.76$ TeV measured with ALICE at the LHC*, J. Phys. **G38**, 124167 (2011), doi:10.1088/0954-3899/38/12/124167.

- [53] U. W. Heinz and P. F. Kolb, *Rapidity dependent momentum anisotropy at RHIC*, J. Phys. **G30**, S1229 (2004), doi:10.1088/0954-3899/30/8/096.

A The ALICE Collaboration

B. Abelev⁷², J. Adam³⁸, D. Adamová⁷⁹, A.M. Adare¹³⁰, M.M. Aggarwal⁸³, G. Aglieri Rinella³⁴, M. Agnello^{100,89}, A.G. Agocs¹²⁹, A. Agostinelli²⁸, Z. Ahammed¹²⁴, N. Ahmad¹⁸, A. Ahmad Masoodi¹⁸, I. Ahmed¹⁶, S.A. Ahn⁶⁵, S.U. Ahn⁶⁵, I. Aimo^{25,100,89}, M. Ajaz¹⁶, A. Akindinov⁵¹, D. Aleksandrov⁹⁵, B. Alessandro¹⁰⁰, D. Alexandre⁹⁷, A. Alici^{102,13}, A. Alkin⁴, J. Alme³⁶, T. Alt⁴⁰, V. Altini³², S. Altinpinar¹⁹, I. Altsybeev¹²⁶, C. Andrei⁷⁵, A. Andronic⁹², V. Anguelov⁸⁸, J. Anielski⁵⁹, C. Anson²⁰, T. Antičić⁹³, F. Antinori¹⁰¹, P. Antonioli¹⁰², L. Aphecetche¹⁰⁸, H. Appelshäuser⁵⁷, N. Arbor⁶⁸, S. Arcelli²⁸, A. Arend⁵⁷, N. Armesto¹⁷, R. Arnaldi¹⁰⁰, T. Aronsson¹³⁰, I.C. Arsene⁹², M. Arslandok⁵⁷, A. Asryan¹²⁶, A. Augustinus³⁴, R. Averbeck⁹², T.C. Awes⁸⁰, J. Äystö⁴³, M.D. Azmi^{18,85}, M. Bach⁴⁰, A. Badalà⁹⁹, Y.W. Baek^{67,41}, R. Bailhache⁵⁷, R. Bala^{86,100}, A. Baldisseri¹⁵, F. Baltasar Dos Santos Pedrosa³⁴, J. Bán⁵², R.C. Baral⁵³, R. Barbera²⁷, F. Barile³², G.G. Barnaföldi¹²⁹, L.S. Barnby⁹⁷, V. Barret⁶⁷, J. Bartke¹¹², M. Basile²⁸, N. Bastid⁶⁷, S. Basu¹²⁴, B. Bathen⁵⁹, G. Batigne¹⁰⁸, B. Batyunya⁶³, P.C. Batzing²², C. Baumann⁵⁷, I.G. Bearden⁷⁷, H. Beck⁵⁷, N.K. Behera⁴⁵, I. Belikov⁶², F. Bellini²⁸, R. Bellwied¹¹⁸, E. Belmont-Moreno⁶¹, G. Bencedi¹²⁹, S. Beole²⁵, I. Berceau⁷⁵, A. Bercuci⁷⁵, Y. Berdnikov⁸¹, D. Berenyi¹²⁹, A.A.E. Bergognon¹⁰⁸, R.A. Bertens⁵⁰, D. Berzano^{25,100}, L. Betev³⁴, A. Bhasin⁸⁶, A.K. Bhati⁸³, J. Bhom¹²², L. Bianchi²⁵, N. Bianchi⁶⁹, C. Bianchin⁵⁰, J. Bielčák³⁸, J. Bielčíková⁷⁹, A. Bilandžić⁷⁷, S. Bjelogrić⁵⁰, F. Blanco¹¹⁸, F. Blanco¹¹, D. Blau⁹⁵, C. Blume⁵⁷, M. Boccioni³⁴, F. Bock^{64,71}, S. Böttger⁵⁶, A. Bogdanov⁷³, H. Bøggild⁷⁷, M. Bogolyubsky⁴⁸, L. Boldizsár¹²⁹, M. Bombara³⁹, J. Book⁵⁷, H. Borel¹⁵, A. Borissov¹²⁸, F. Bossu⁸⁵, M. Botje⁷⁸, E. Botta²⁵, E. Braidot⁷¹, P. Braun-Munzinger⁹², M. Bregant¹⁰⁸, T. Breitner⁵⁶, T.A. Broker⁵⁷, T.A. Browning⁹⁰, M. Broz³⁷, R. Brun³⁴, E. Bruna^{25,100}, G.E. Bruno³², D. Budnikov⁹⁴, H. Buesching⁵⁷, S. Bufalino^{25,100}, P. Buncic³⁴, O. Busch⁸⁸, Z. Buthelezi⁸⁵, D. Caffarri^{29,101}, X. Cai⁸, H. Caines¹³⁰, A. Caliva⁵⁰, E. Calvo Villar⁹⁸, P. Camerini²³, V. Canoa Roman¹², G. Cara Romeo¹⁰², F. Carena³⁴, W. Carena³⁴, N. Carlin Filho¹¹⁵, F. Carminati³⁴, A. Casanova Díaz⁶⁹, J. Castillo Castellanos¹⁵, J.F. Castillo Hernandez⁹², E.A.R. Casula²⁴, V. Catanescu⁷⁵, C. Cavicchioli³⁴, C. Ceballos Sanchez¹⁰, J. Cepila³⁸, P. Cerello¹⁰⁰, B. Chang^{43,132}, S. Chapeland³⁴, J.L. Charvet¹⁵, S. Chattopadhyay¹²⁴, S. Chattopadhyay⁹⁶, M. Cherney⁸², C. Cheshkov^{34,117}, B. Cheynis¹¹⁷, V. Chibante Barroso³⁴, D.D. Chinellato¹¹⁸, P. Chochula³⁴, M. Chojnacki⁷⁷, S. Choudhury¹²⁴, P. Christakoglou⁷⁸, C.H. Christensen⁷⁷, P. Christiansen³³, T. Chujo¹²², S.U. Chung⁹¹, C. Cicalo¹⁰³, L. Cifarelli^{28,13}, F. Cindolo¹⁰², J. Cleymans⁸⁵, F. Colamaria³², D. Colella³², A. Collu²⁴, G. Conesa Balbastre⁶⁸, Z. Conesa del Valle^{34,47}, M.E. Connors¹³⁰, G. Contin²³, J.G. Contreras¹², T.M. Cormier¹²⁸, Y. Corrales Morales²⁵, P. Cortese³¹, I. Cortés Maldonado³, M.R. Cosentino⁷¹, F. Costa³⁴, M.E. Cotallo¹¹, E. Crescio¹², P. Crochet⁶⁷, E. Cruz Alaniz⁷⁸, R. Cruz Albino¹², E. Cuautle⁶⁰, L. Cunqueiro⁶⁹, T.R. Czopowicz¹²⁷, A. Dainese^{29,101}, R. Dang⁸, A. Danu⁵⁵, D. Das⁹⁶, I. Das⁴⁷, S. Das⁵, K. Das⁹⁶, A. Dash¹¹⁶, S. Dash⁴⁵, S. De¹²⁴, G.O.V. de Barros¹¹⁵, A. De Caro^{30,13}, G. de Cataldo¹⁰⁵, J. de Cuveland⁴⁰, A. De Falco²⁴, D. De Gruttola^{30,13}, H. Delagrange¹⁰⁸, A. Deloff⁷⁴, N. De Marco¹⁰⁰, E. Dénes¹²⁹, S. De Pasquale³⁰, A. Deppman¹¹⁵, G. D'Erasmus³², R. de Rooij⁵⁰, M.A. Diaz Corchero¹¹, D. Di Bari³², T. Dietel⁵⁹, C. Di Giglio³², S. Di Liberto¹⁰⁶, A. Di Mauro³⁴, P. Di Nezza⁶⁹, R. Divià³⁴, Ø. Djuvsland¹⁹, A. Dobrin^{128,33,50}, T. Dobrowolski⁷⁴, B. Dönigus^{92,57}, O. Dordic²², A.K. Dubey¹²⁴, A. Dubla⁵⁰, L. Ducroux¹¹⁷, P. Dupieux⁶⁷, A.K. Dutta Majumdar⁹⁶, D. Elia¹⁰⁵, B.G. Elwood¹⁴, D. Emschermann⁵⁹, H. Engel⁵⁶, B. Erasmus^{34,108}, H.A. Erdal³⁶, D. Eschweiler⁴⁰, B. Espagnon⁴⁷, M. Estienne¹⁰⁸, S. Esumi¹²², D. Evans⁹⁷, S. Evdokimov⁴⁸, G. Eyyubova²², D. Fabris^{29,101}, J. Faivre⁶⁸, D. Falchieri²⁸, A. Fantoni⁶⁹, M. Fasel⁸⁸, D. Fehler¹⁹, L. Feldkamp⁵⁹, D. Felea⁵⁵, A. Feliciello¹⁰⁰, B. Fenton-Olsen⁷¹, G. Feofilov¹²⁶, A. Fernández Téllez³, A. Ferretti²⁵, A. Festanti²⁹, J. Figiel¹¹², M.A.S. Figueredo¹¹⁵, S. Filchagin⁹⁴, D. Finogeev⁴⁹, F.M. Fionda³², E.M. Fiore³², E. Floratos⁸⁴, M. Floris³⁴, S. Foertsch⁸⁵, P. Foka⁹², S. Fokin⁹⁵, E. Fragiaco¹⁰⁴, A. Francescon^{34,29}, U. Frankendorf⁹², U. Fuchs³⁴, C. Furget⁶⁸, M. Fusco Girard³⁰, J.J. Gaardhøje⁷⁷, M. Gagliardi²⁵, A. Gago⁹⁸, M. Gallio²⁵, D.R. Gangadharan²⁰, P. Ganoti⁸⁰, C. Garabatos⁹², E. Garcia-Solis¹⁴, C. Gargiulo³⁴, I. Garishvili⁷², J. Gerhard⁴⁰, M. Germain¹⁰⁸, A. Gheata³⁴, M. Gheata^{55,34}, B. Ghidini³², P. Ghosh¹²⁴, P. Gianotti⁶⁹, P. Giubellino³⁴, E. Gladysz-Dziadus¹¹², P. Glässel⁸⁸, L. Goerlich¹¹², R. Gomez^{114,12}, E.G. Ferreira¹⁷, P. González-Zamora¹¹, S. Gorbunov⁴⁰, A. Goswami⁸⁷, S. Gotovac¹¹⁰, L.K. Graczykowski¹²⁷, R. Graczyk⁸⁸, A. Grelli⁵⁰, A. Grigoras³⁴, C. Grigoras³⁴, V. Grigoriev⁷³, A. Grigoryan², S. Grigoryan⁶³, B. Grinyov⁴, N. Grion¹⁰⁴, P. Gros³³, J.F. Grosse-Oetringhaus³⁴, J.-Y. Grossiord¹¹⁷, R. Grosso³⁴, F. Guber⁴⁹, R. Guernane⁶⁸, B. Guerzoni²⁸, M. Guilbaud¹¹⁷, K. Gulbrandsen⁷⁷, H. Gulkanyan², T. Gunji¹²¹, A. Gupta⁸⁶, R. Gupta⁸⁶, R. Haake⁵⁹, Ø. Haaland¹⁹, C. Hadjidakis⁴⁷, M. Haiduc⁵⁵, H. Hamagaki¹²¹, G. Hamar¹²⁹, B.H. Han²¹, L.D. Hanratty⁹⁷, A. Hansen⁷⁷, J.W. Harris¹³⁰, A. Harton¹⁴, D. Hatzifotiadou¹⁰², S. Hayashi¹²¹, A. Hayrapetyan^{34,2}, S.T. Heckel⁵⁷, M. Heide⁵⁹, H. Helstrup³⁶, A. Herghelegiu⁷⁵, G. Herrera Corral¹², N. Herrmann⁸⁸, B.A. Hess¹²³, K.F. Hetland³⁶, B. Hicks¹³⁰, B. Hippolyte⁶², Y. Hori¹²¹, P. Hristov³⁴,

I. Hřivnáčová⁴⁷, M. Huang¹⁹, T.J. Humanic²⁰, D.S. Hwang²¹, R. Ichou⁶⁷, R. Ilkaev⁹⁴, I. Ilkiv⁷⁴, M. Inaba¹²², E. Incani²⁴, P.G. Innocenti³⁴, G.M. Innocenti²⁵, C. Ionita³⁴, M. Ippolitov⁹⁵, M. Irfan¹⁸, V. Ivanov⁸¹, M. Ivanov⁹², A. Ivanov¹²⁶, O. Ivanytskyi⁴, A. Jachołkowski²⁷, P. M. Jacobs⁷¹, C. Jahnke¹¹⁵, H.J. Jang⁶⁵, M.A. Janik¹²⁷, P.H.S.Y. Jayarathna¹¹⁸, S. Jena⁴⁵, D.M. Jha¹²⁸, R.T. Jimenez Bustamante⁶⁰, P.G. Jones⁹⁷, H. Jung⁴¹, A. Jusko⁹⁷, A.B. Kaidalov⁵¹, S. Kalcher⁴⁰, P. Kaliňák⁵², T. Kalliokoski⁴³, A. Kalweit³⁴, J.H. Kang¹³², V. Kaplin⁷³, S. Kar¹²⁴, A. Karasu Uysal⁶⁶, O. Karavichev⁴⁹, T. Karavicheva⁴⁹, E. Karpechev⁴⁹, A. Kazantsev⁹⁵, U. Kebschull⁵⁶, R. Keidel¹³³, B. Ketzer^{57,111}, M.M. Khan¹⁸, P. Khan⁹⁶, K. H. Khan¹⁶, S.A. Khan¹²⁴, A. Khanzadeev⁸¹, Y. Kharlov⁴⁸, B. Kileng³⁶, J.S. Kim⁴¹, B. Kim¹³², T. Kim¹³², D.J. Kim⁴³, S. Kim²¹, M. Kim⁴¹, D.W. Kim^{41,65}, J.H. Kim²¹, M. Kim¹³², S. Kirsch⁴⁰, I. Kisel⁴⁰, S. Kiselev⁵¹, A. Kisiel¹²⁷, G. Kiss¹²⁹, J.L. Klay⁷, J. Klein⁸⁸, C. Klein-Bösing⁵⁹, M. Kliemant⁵⁷, A. Kluge³⁴, M.L. Knichel⁹², A.G. Knospe¹¹³, M.K. Köhler⁹², T. Kollegger⁴⁰, A. Kolojvari¹²⁶, M. Kompaniets¹²⁶, V. Kondratiev¹²⁶, N. Kondratyeva⁷³, A. Konevskikh⁴⁹, V. Kovalenko¹²⁶, M. Kowalski¹¹², S. Kox⁶⁸, G. Koyithatta Meethalevedu⁴⁵, J. Kral⁴³, I. Králik⁵², F. Kramer⁵⁷, A. Kravčáková³⁹, M. Krelina³⁸, M. Kretz⁴⁰, M. Krivda^{97,52}, F. Krizek^{43,38,79}, M. Krus³⁸, E. Kryshen⁸¹, M. Krzewicki⁹², V. Kucera⁷⁹, Y. Kucheriaev⁹⁵, T. Kugathasan³⁴, C. Kuhn⁶², P.G. Kuijjer⁷⁸, I. Kulakov⁵⁷, J. Kumar⁴⁵, P. Kurashvili⁷⁴, A. Kurepin⁴⁹, A.B. Kurepin⁴⁹, A. Kuryakin⁹⁴, S. Kushpil⁷⁹, V. Kushpil⁷⁹, H. Kvaerno²², M.J. Kweon⁸⁸, Y. Kwon¹³², P. Ladrón de Guevara⁶⁰, C. Lagana Fernandes¹¹⁵, I. Lakomov⁴⁷, R. Langoy¹²⁵, S.L. La Pointe⁵⁰, C. Lara⁵⁶, A. Lardeux¹⁰⁸, P. La Rocca²⁷, R. Lea²³, M. Lechman³⁴, G.R. Lee⁹⁷, S.C. Lee⁴¹, I. Legrand³⁴, J. Lehnert⁵⁷, R.C. Lemmon¹⁰⁷, M. Lenhardt⁹², V. Lenti¹⁰⁵, H. León⁶¹, M. Leoncino²⁵, I. León Monzón¹¹⁴, P. Lévai¹²⁹, S. Li^{67,8}, J. Lien^{19,125}, R. Lietava⁹⁷, S. Lindal²², V. Lindenstruth⁴⁰, C. Lippmann^{92,34}, M.A. Lisa²⁰, H.M. Ljunggren³³, D.F. Lodato⁵⁰, P.I. Loenne¹⁹, V.R. Loggins¹²⁸, V. Loginov⁷³, D. Lohner⁸⁸, C. Loizides⁷¹, K.K. Loo⁴³, X. Lopez⁶⁷, E. López Torres¹⁰, G. Løvhøiden²², X.-G. Lu⁸⁸, P. Luettig⁵⁷, M. Lunardon²⁹, J. Luo⁸, G. Luparello⁵⁰, C. Luzzi³⁴, R. Ma¹³⁰, K. Ma⁸, D.M. Madagodahettige-Don¹¹⁸, A. Maevskaya⁴⁹, M. Mager^{58,34}, D.P. Mahapatra⁵³, A. Maire⁸⁸, M. Malaev⁸¹, I. Maldonado Cervantes⁶⁰, L. Malinina^{63,ii}, D. Mal'Kevich⁵¹, P. Malzacher⁹², A. Mamonov⁹⁴, L. Manceau¹⁰⁰, L. Mangotra⁸⁶, V. Manko⁹⁵, F. Manso⁶⁷, V. Manzari¹⁰⁵, M. Marchisone^{67,25}, J. Mareš⁵⁴, G.V. Margagliotti^{23,104}, A. Margotti¹⁰², A. Marín⁹², C. Markert^{34,113}, M. Marquard⁵⁷, I. Martashvili¹²⁰, N.A. Martin⁹², J. Martin Blanco¹⁰⁸, P. Martinengo³⁴, M.I. Martínez³, G. Martínez García¹⁰⁸, Y. Martynov⁴, A. Mas¹⁰⁸, S. Masciocchi⁹², M. Maserà²⁵, A. Masoni¹⁰³, L. Massacrier¹⁰⁸, A. Mastroserio³², A. Matyja¹¹², C. Mayer¹¹², J. Mazer¹²⁰, R. Mazumder⁴⁶, M.A. Mazzoni¹⁰⁶, F. Meddi²⁶, A. Menchaca-Rocha⁶¹, J. Mercado Pérez⁸⁸, M. Meres³⁷, Y. Miake¹²², K. Mikhaylov^{63,51}, L. Milano^{34,25}, J. Milosevic^{22,iii}, A. Mischke⁵⁰, A.N. Mishra^{87,46}, D. Miśkowiec⁹², C. Mitu⁵⁵, J. Mlynarz¹²⁸, B. Mohanty^{124,76}, L. Molnar^{129,62}, L. Montaña Zetina¹², M. Monteno¹⁰⁰, E. Montes¹¹, T. Moon¹³², M. Morando²⁹, D.A. Moreira De Godoy¹¹⁵, S. Moretto²⁹, A. Morreale⁴³, A. Morsch³⁴, V. Muccifora⁶⁹, E. Mudnic¹¹⁰, S. Muhuri¹²⁴, M. Mukherjee¹²⁴, H. Müller³⁴, M.G. Munhoz¹¹⁵, S. Murray⁸⁵, L. Musa³⁴, J. Musinsky⁵², B.K. Nandi⁴⁵, R. Nania¹⁰², E. Nappi¹⁰⁵, M. Nasar¹, C. Nattrass¹²⁰, T.K. Nayak¹²⁴, S. Nazarenko⁹⁴, A. Nedosekin⁵¹, M. Nicassio^{32,92}, M. Niculescu^{55,34}, B.S. Nielsen⁷⁷, S. Nikolaev⁹⁵, V. Nikolic⁹³, V. Nikulin⁸¹, S. Nikulin⁹⁵, B.S. Nilsen⁸², M.S. Nilsson²², F. Noferini^{102,13}, P. Nomokonov⁶³, G. Nooren⁵⁰, A. Nyanin⁹⁵, A. Nyatha⁴⁵, C. Nygaard⁷⁷, J. Nystrand¹⁹, A. Ochirov¹²⁶, H. Oeschler^{58,34,88}, S.K. Oh⁴¹, S. Oh¹³⁰, L. Olah¹²⁹, J. Oleniacz¹²⁷, A.C. Oliveira Da Silva¹¹⁵, J. Onderwaater⁹², C. Oppedisano¹⁰⁰, A. Ortiz Velasquez^{33,60}, A. Oskarsson³³, P. Ostrowski¹²⁷, J. Otwinowski⁹², K. Oyama⁸⁸, K. Ozawa¹²¹, Y. Pachmayer⁸⁸, M. Pachr³⁸, F. Padilla²⁵, P. Pagano³⁰, G. Paic⁶⁰, F. Painke⁴⁰, C. Pajares¹⁷, S.K. Pal¹²⁴, A. Palaha⁹⁷, A. Palmeri⁹⁹, V. Papikyan², G.S. Pappalardo⁹⁹, W.J. Park⁹², A. Passfeld⁵⁹, D.I. Patalakha⁴⁸, V. Paticchio¹⁰⁵, B. Paul⁹⁶, A. Pavlinov¹²⁸, T. Pawlak¹²⁷, T. Peitzmann⁵⁰, H. Pereira Da Costa¹⁵, E. Pereira De Oliveira Filho¹¹⁵, D. Peresunko⁹⁵, C.E. Pérez Lara⁷⁸, D. Perrino³², W. Peryt^{127,i}, A. Pesci¹⁰², Y. Pestov⁶, V. Petráček³⁸, M. Petran³⁸, M. Petris⁷⁵, P. Petrov⁹⁷, M. Petrovici⁷⁵, C. Petta²⁷, S. Piano¹⁰⁴, M. Pikna³⁷, P. Pillot¹⁰⁸, O. Pinazza³⁴, L. Pinsky¹¹⁸, N. Pitz⁵⁷, D.B. Piyarathna¹¹⁸, M. Planinic⁹³, M. Płoskoń⁷¹, J. Pluta¹²⁷, T. Pocheptsov⁶³, S. Pochybova¹²⁹, P.L.M. Podesta-Lerma¹¹⁴, M.G. Poghosyan³⁴, K. Polák⁵⁴, B. Polichtchouk⁴⁸, N. Poljak^{50,93}, A. Pop⁷⁵, S. Porteboeuf-Houssais⁶⁷, V. Pospíšil³⁸, B. Potukuchi⁸⁶, S.K. Prasad¹²⁸, R. Preghenella^{102,13}, F. Prino¹⁰⁰, C.A. Pruneau¹²⁸, I. Pshenichnov⁴⁹, G. Puddu²⁴, V. Punin⁹⁴, J. Putschke¹²⁸, H. Qvigstad²², A. Rachevski¹⁰⁴, A. Rademakers³⁴, J. Rak⁴³, A. Rakotozafindrabe¹⁵, L. Ramello³¹, S. Raniwala⁸⁷, R. Raniwala⁸⁷, S.S. Räsänen⁴³, B.T. Rascanu⁵⁷, D. Rathee⁸³, W. Rauch³⁴, A.W. Rauf¹⁶, V. Razazi²⁴, K.F. Read¹²⁰, J.S. Real⁶⁸, K. Redlich^{74,iv}, R.J. Reed¹³⁰, A. Rehman¹⁹, P. Reichelt⁵⁷, M. Reicher⁵⁰, F. Reidt⁸⁸, R. Renfordt⁵⁷, A.R. Reolon⁶⁹, A. Reshetin⁴⁹, F. Rettig⁴⁰, J.-P. Revol³⁴, K. Reygers⁸⁸, L. Riccati¹⁰⁰, R.A. Ricci⁷⁰, T. Richert³³, M. Richter²², P. Riedler³⁴, W. Riegler³⁴, F. Riggi^{27,99}, A. Rivetti¹⁰⁰, M. Rodríguez Cahuantzi³, A. Rodríguez Manso⁷⁸, K. Røed^{19,22}, E. Rogochaya⁶³, D. Rohr⁴⁰, D. Röhrich¹⁹, R. Romita^{92,107},

F. Ronchetti⁶⁹, P. Rosnet⁶⁷, S. Rossegger³⁴, A. Rossi³⁴, P. Roy⁹⁶, C. Roy⁶², A.J. Rubio Montero¹¹, R. Rui²³, R. Russo²⁵, E. Ryabinkin⁹⁵, A. Rybicki¹¹², S. Sadovsky⁴⁸, K. Šafařík³⁴, R. Sahoo⁴⁶, P.K. Sahu⁵³, J. Saini¹²⁴, H. Sakaguchi⁴⁴, S. Sakai^{71,69}, D. Sakata¹²², C.A. Salgado¹⁷, J. Salzwedel²⁰, S. Sambyal⁸⁶, V. Samsonov⁸¹, X. Sanchez Castro⁶², L. Šándor⁵², A. Sandoval⁶¹, M. Sano¹²², G. Santagati²⁷, R. Santoro^{34,13}, D. Sarkar¹²⁴, E. Scapparone¹⁰², F. Scarlassara²⁹, R.P. Scharenberg⁹⁰, C. Schiaua⁷⁵, R. Schicker⁸⁸, C. Schmidt⁹², H.R. Schmidt¹²³, S. Schuchmann⁵⁷, J. Schukraft³⁴, M. Schulc³⁸, T. Schuster¹³⁰, Y. Schutz^{34,108}, K. Schwarz⁹², K. Schweda⁹², G. Scioli²⁸, E. Scomparin¹⁰⁰, P.A. Scott⁹⁷, R. Scott¹²⁰, G. Segato²⁹, I. Selyuzhenkov⁹², S. Senyukov⁶², J. Seo⁹¹, S. Serici²⁴, E. Serradilla^{11,61}, A. Sevcenco⁵⁵, A. Shabetai¹⁰⁸, G. Shabratova⁶³, R. Shahoyan³⁴, N. Sharma¹²⁰, S. Sharma⁸⁶, S. Rohni⁸⁶, K. Shigaki⁴⁴, K. Shtejer¹⁰, Y. Sibiriak⁹⁵, S. Siddhanta¹⁰³, T. Siemiarczuk⁷⁴, D. Silvermyr⁸⁰, C. Silvestre⁶⁸, G. Simatovic^{60,93}, G. Simonetti³⁴, R. Singaraju¹²⁴, R. Singh⁸⁶, S. Singha^{124,76}, V. Singhal¹²⁴, T. Sinha⁹⁶, B.C. Sinha¹²⁴, B. Sitar³⁷, M. Sitta³¹, T.B. Skaali²², K. Skjerdal¹⁹, R. Smakal³⁸, N. Smirnov¹³⁰, R.J.M. Snellings⁵⁰, C. Sogaard³³, R. Soltz⁷², J. Song⁹¹, M. Song¹³², C. Soos³⁴, F. Soramel²⁹, M. Spacek³⁸, I. Sputowska¹¹², M. Spyropoulou-Stassinaki⁸⁴, B.K. Srivastava⁹⁰, J. Stachel⁸⁸, I. Stan⁵⁵, G. Stefanek⁷⁴, M. Steinpreis²⁰, E. Stenlund³³, G. Steyn⁸⁵, J.H. Stiller⁸⁸, D. Stocco¹⁰⁸, M. Stolpovskiy⁴⁸, P. Strmen³⁷, A.A.P. Suaide¹¹⁵, M.A. Subieta Vásquez²⁵, T. Sugitate⁴⁴, C. Suire⁴⁷, M. Suleymanov¹⁶, R. Sultanov⁵¹, M. Šumbera⁷⁹, T. Susa⁹³, T.J.M. Symons⁷¹, A. Szanto de Toledo¹¹⁵, I. Szarka³⁷, A. Szczepankiewicz³⁴, M. Szymański¹²⁷, J. Takahashi¹¹⁶, M.A. Tangaro³², J.D. Tapia Takaki⁴⁷, A. Tarantola Piloni⁵⁷, A. Tarazona Martinez³⁴, A. Tauro³⁴, G. Tejada Muñoz³, A. Telesca³⁴, A. Ter Minasyan⁹⁵, C. Terrevoli³², J. Thäder⁹², D. Thomas⁵⁰, R. Tieulent¹¹⁷, A.R. Timmins¹¹⁸, D. Tlusty³⁸, A. Toia^{40,29,101}, H. Torii¹²¹, L. Toscano¹⁰⁰, V. Trubnikov⁴, D. Truesdale²⁰, W.H. Trzaska⁴³, T. Tsuji¹²¹, A. Tumkin⁹⁴, R. Turrisi¹⁰¹, T.S. Tveter²², J. Ulery⁵⁷, K. Ullaland¹⁹, J. Ulrich^{64,56}, A. Uras¹¹⁷, G.M. Urciuoli¹⁰⁶, G.L. Usai²⁴, M. Vajzer^{38,79}, M. Vala^{63,52}, L. Valencia Palomo⁴⁷, S. Vallero²⁵, P. Vande Vyvre³⁴, J.W. Van Hoorne³⁴, M. van Leeuwen⁵⁰, L. Vannucci⁷⁰, A. Vargas³, R. Varma⁴⁵, M. Vasileiou⁸⁴, A. Vasiliev⁹⁵, V. Vechernin¹²⁶, M. Veldhoen⁵⁰, M. Venaruzzo²³, E. Vercellin²⁵, S. Vergara³, R. Vernet⁹, M. Verweij^{128,50}, L. Vickovic¹¹⁰, G. Viesti²⁹, J. Viinikainen⁴³, Z. Vilakazi⁸⁵, O. Villalobos Baillie⁹⁷, Y. Vinogradov⁹⁴, A. Vinogradov⁹⁵, L. Vinogradov¹²⁶, T. Virgili³⁰, Y.P. Viyogi¹²⁴, A. Vodopyanov⁶³, M.A. Völkl⁸⁸, K. Voloshin⁵¹, S. Voloshin¹²⁸, G. Volpe³⁴, B. von Haller³⁴, I. Vorobyev¹²⁶, D. Vranic^{92,34}, J. Vrláková³⁹, B. Vulpescu⁶⁷, A. Vyushin⁹⁴, B. Wagner¹⁹, V. Wagner³⁸, J. Wagner⁹², Y. Wang⁸, M. Wang⁸, Y. Wang⁸⁸, D. Watanabe¹²², K. Watanabe¹²², M. Weber¹¹⁸, J.P. Wessels⁵⁹, U. Westerhoff⁵⁹, J. Wiechula¹²³, D. Wielanek¹²⁷, J. Wikne²², M. Wilde⁵⁹, G. Wilk⁷⁴, J. Wilkinson⁸⁸, M.C.S. Williams¹⁰², M. Winn⁸⁸, B. Windelband⁸⁸, C. Xiang⁸, C.G. Yaldo¹²⁸, Y. Yamaguchi¹²¹, H. Yang^{15,50}, S. Yang¹⁹, P. Yang⁸, S. Yano⁴⁴, S. Yasnopolskiy⁹⁵, J. Yi⁹¹, Z. Yin⁸, I.-K. Yoo⁹¹, J. Yoon¹³², I. Yushmanov⁹⁵, V. Zaccaro⁷⁷, C. Zach³⁸, C. Zampolli¹⁰², S. Zaporozhets⁶³, A. Zarochentsev¹²⁶, P. Závada⁵⁴, N. Zaviyalov⁹⁴, H. Zbroszczyk¹²⁷, P. Zelnicsek⁵⁶, I.S. Zgura⁵⁵, M. Zhalov⁸¹, Y. Zhang⁸, X. Zhang^{71,67,8}, F. Zhang⁸, H. Zhang⁸, Y. Zhou⁵⁰, F. Zhou⁸, D. Zhou⁸, H. Zhu⁸, X. Zhu⁸, J. Zhu⁸, J. Zhu⁸, A. Zichichi^{28,13}, A. Zimmermann⁸⁸, G. Zinovjev⁴, Y. Zoccarato¹¹⁷, M. Zynovyev⁴, M. Zyzak⁵⁷

Affiliation notes

- ⁱ Deceased
- ⁱⁱ Also at: M.V.Lomonosov Moscow State University, D.V.Skobeltzyn Institute of Nuclear Physics, Moscow, Russia
- ⁱⁱⁱ Also at: University of Belgrade, Faculty of Physics and "Vinča" Institute of Nuclear Sciences, Belgrade, Serbia
- ^{iv} Also at: Institute of Theoretical Physics, University of Wrocław, Wrocław, Poland

Collaboration Institutes

- ¹ Academy of Scientific Research and Technology (ASRT), Cairo, Egypt
- ² A. I. Alikhanyan National Science Laboratory (Yerevan Physics Institute) Foundation, Yerevan, Armenia
- ³ Benemérita Universidad Autónoma de Puebla, Puebla, Mexico
- ⁴ Bogolyubov Institute for Theoretical Physics, Kiev, Ukraine
- ⁵ Bose Institute, Department of Physics and Centre for Astroparticle Physics and Space Science (CAPSS), Kolkata, India
- ⁶ Budker Institute for Nuclear Physics, Novosibirsk, Russia
- ⁷ California Polytechnic State University, San Luis Obispo, California, United States
- ⁸ Central China Normal University, Wuhan, China

- ⁹ Centre de Calcul de l'IN2P3, Villeurbanne, France
- ¹⁰ Centro de Aplicaciones Tecnológicas y Desarrollo Nuclear (CEADEN), Havana, Cuba
- ¹¹ Centro de Investigaciones Energéticas Medioambientales y Tecnológicas (CIEMAT), Madrid, Spain
- ¹² Centro de Investigación y de Estudios Avanzados (CINVESTAV), Mexico City and Mérida, Mexico
- ¹³ Centro Fermi - Museo Storico della Fisica e Centro Studi e Ricerche "Enrico Fermi", Rome, Italy
- ¹⁴ Chicago State University, Chicago, United States
- ¹⁵ Commissariat à l'Energie Atomique, IRFU, Saclay, France
- ¹⁶ COMSATS Institute of Information Technology (CIIT), Islamabad, Pakistan
- ¹⁷ Departamento de Física de Partículas and IGFAE, Universidad de Santiago de Compostela, Santiago de Compostela, Spain
- ¹⁸ Department of Physics Aligarh Muslim University, Aligarh, India
- ¹⁹ Department of Physics and Technology, University of Bergen, Bergen, Norway
- ²⁰ Department of Physics, Ohio State University, Columbus, Ohio, United States
- ²¹ Department of Physics, Sejong University, Seoul, South Korea
- ²² Department of Physics, University of Oslo, Oslo, Norway
- ²³ Dipartimento di Fisica dell'Università and Sezione INFN, Trieste, Italy
- ²⁴ Dipartimento di Fisica dell'Università and Sezione INFN, Cagliari, Italy
- ²⁵ Dipartimento di Fisica dell'Università and Sezione INFN, Turin, Italy
- ²⁶ Dipartimento di Fisica dell'Università 'La Sapienza' and Sezione INFN, Rome, Italy
- ²⁷ Dipartimento di Fisica e Astronomia dell'Università and Sezione INFN, Catania, Italy
- ²⁸ Dipartimento di Fisica e Astronomia dell'Università and Sezione INFN, Bologna, Italy
- ²⁹ Dipartimento di Fisica e Astronomia dell'Università and Sezione INFN, Padova, Italy
- ³⁰ Dipartimento di Fisica 'E.R. Caianiello' dell'Università and Gruppo Collegato INFN, Salerno, Italy
- ³¹ Dipartimento di Scienze e Innovazione Tecnologica dell'Università del Piemonte Orientale and Gruppo Collegato INFN, Alessandria, Italy
- ³² Dipartimento Interateneo di Fisica 'M. Merlin' and Sezione INFN, Bari, Italy
- ³³ Division of Experimental High Energy Physics, University of Lund, Lund, Sweden
- ³⁴ European Organization for Nuclear Research (CERN), Geneva, Switzerland
- ³⁵ Fachhochschule Köln, Köln, Germany
- ³⁶ Faculty of Engineering, Bergen University College, Bergen, Norway
- ³⁷ Faculty of Mathematics, Physics and Informatics, Comenius University, Bratislava, Slovakia
- ³⁸ Faculty of Nuclear Sciences and Physical Engineering, Czech Technical University in Prague, Prague, Czech Republic
- ³⁹ Faculty of Science, P.J. Šafárik University, Košice, Slovakia
- ⁴⁰ Frankfurt Institute for Advanced Studies, Johann Wolfgang Goethe-Universität Frankfurt, Frankfurt, Germany
- ⁴¹ Gangneung-Wonju National University, Gangneung, South Korea
- ⁴² Gauhati University, Department of Physics, Guwahati, India
- ⁴³ Helsinki Institute of Physics (HIP) and University of Jyväskylä, Jyväskylä, Finland
- ⁴⁴ Hiroshima University, Hiroshima, Japan
- ⁴⁵ Indian Institute of Technology Bombay (IIT), Mumbai, India
- ⁴⁶ Indian Institute of Technology Indore, Indore, India (IITI)
- ⁴⁷ Institut de Physique Nucléaire d'Orsay (IPNO), Université Paris-Sud, CNRS-IN2P3, Orsay, France
- ⁴⁸ Institute for High Energy Physics, Protvino, Russia
- ⁴⁹ Institute for Nuclear Research, Academy of Sciences, Moscow, Russia
- ⁵⁰ Nikhef, National Institute for Subatomic Physics and Institute for Subatomic Physics of Utrecht University, Utrecht, Netherlands
- ⁵¹ Institute for Theoretical and Experimental Physics, Moscow, Russia
- ⁵² Institute of Experimental Physics, Slovak Academy of Sciences, Košice, Slovakia
- ⁵³ Institute of Physics, Bhubaneswar, India
- ⁵⁴ Institute of Physics, Academy of Sciences of the Czech Republic, Prague, Czech Republic
- ⁵⁵ Institute of Space Sciences (ISS), Bucharest, Romania
- ⁵⁶ Institut für Informatik, Johann Wolfgang Goethe-Universität Frankfurt, Frankfurt, Germany
- ⁵⁷ Institut für Kernphysik, Johann Wolfgang Goethe-Universität Frankfurt, Frankfurt, Germany
- ⁵⁸ Institut für Kernphysik, Technische Universität Darmstadt, Darmstadt, Germany
- ⁵⁹ Institut für Kernphysik, Westfälische Wilhelms-Universität Münster, Münster, Germany

- 60 Instituto de Ciencias Nucleares, Universidad Nacional Autónoma de México, Mexico City, Mexico
- 61 Instituto de Física, Universidad Nacional Autónoma de México, Mexico City, Mexico
- 62 Institut Pluridisciplinaire Hubert Curien (IPHC), Université de Strasbourg, CNRS-IN2P3, Strasbourg, France
- 63 Joint Institute for Nuclear Research (JINR), Dubna, Russia
- 64 Kirchhoff-Institut für Physik, Ruprecht-Karls-Universität Heidelberg, Heidelberg, Germany
- 65 Korea Institute of Science and Technology Information, Daejeon, South Korea
- 66 KTO Karatay University, Konya, Turkey
- 67 Laboratoire de Physique Corpusculaire (LPC), Clermont Université, Université Blaise Pascal, CNRS-IN2P3, Clermont-Ferrand, France
- 68 Laboratoire de Physique Subatomique et de Cosmologie (LPSC), Université Joseph Fourier, CNRS-IN2P3, Institut Polytechnique de Grenoble, Grenoble, France
- 69 Laboratori Nazionali di Frascati, INFN, Frascati, Italy
- 70 Laboratori Nazionali di Legnaro, INFN, Legnaro, Italy
- 71 Lawrence Berkeley National Laboratory, Berkeley, California, United States
- 72 Lawrence Livermore National Laboratory, Livermore, California, United States
- 73 Moscow Engineering Physics Institute, Moscow, Russia
- 74 National Centre for Nuclear Studies, Warsaw, Poland
- 75 National Institute for Physics and Nuclear Engineering, Bucharest, Romania
- 76 National Institute of Science Education and Research, Bhubaneswar, India
- 77 Niels Bohr Institute, University of Copenhagen, Copenhagen, Denmark
- 78 Nikhef, National Institute for Subatomic Physics, Amsterdam, Netherlands
- 79 Nuclear Physics Institute, Academy of Sciences of the Czech Republic, Řež u Prahy, Czech Republic
- 80 Oak Ridge National Laboratory, Oak Ridge, Tennessee, United States
- 81 Petersburg Nuclear Physics Institute, Gatchina, Russia
- 82 Physics Department, Creighton University, Omaha, Nebraska, United States
- 83 Physics Department, Panjab University, Chandigarh, India
- 84 Physics Department, University of Athens, Athens, Greece
- 85 Physics Department, University of Cape Town and iThemba LABS, National Research Foundation, Somerset West, South Africa
- 86 Physics Department, University of Jammu, Jammu, India
- 87 Physics Department, University of Rajasthan, Jaipur, India
- 88 Physikalisches Institut, Ruprecht-Karls-Universität Heidelberg, Heidelberg, Germany
- 89 Politecnico di Torino, Turin, Italy
- 90 Purdue University, West Lafayette, Indiana, United States
- 91 Pusan National University, Pusan, South Korea
- 92 Research Division and ExtreMe Matter Institute EMMI, GSI Helmholtzzentrum für Schwerionenforschung, Darmstadt, Germany
- 93 Rudjer Bošković Institute, Zagreb, Croatia
- 94 Russian Federal Nuclear Center (VNIIEF), Sarov, Russia
- 95 Russian Research Centre Kurchatov Institute, Moscow, Russia
- 96 Saha Institute of Nuclear Physics, Kolkata, India
- 97 School of Physics and Astronomy, University of Birmingham, Birmingham, United Kingdom
- 98 Sección Física, Departamento de Ciencias, Pontificia Universidad Católica del Perú, Lima, Peru
- 99 Sezione INFN, Catania, Italy
- 100 Sezione INFN, Turin, Italy
- 101 Sezione INFN, Padova, Italy
- 102 Sezione INFN, Bologna, Italy
- 103 Sezione INFN, Cagliari, Italy
- 104 Sezione INFN, Trieste, Italy
- 105 Sezione INFN, Bari, Italy
- 106 Sezione INFN, Rome, Italy
- 107 Nuclear Physics Group, STFC Daresbury Laboratory, Daresbury, United Kingdom
- 108 SUBATECH, Ecole des Mines de Nantes, Université de Nantes, CNRS-IN2P3, Nantes, France
- 109 Suranaree University of Technology, Nakhon Ratchasima, Thailand
- 110 Technical University of Split FESB, Split, Croatia

- 111 Technische Universität München, Munich, Germany
- 112 The Henryk Niewodniczanski Institute of Nuclear Physics, Polish Academy of Sciences, Cracow, Poland
- 113 The University of Texas at Austin, Physics Department, Austin, TX, United States
- 114 Universidad Autónoma de Sinaloa, Culiacán, Mexico
- 115 Universidade de São Paulo (USP), São Paulo, Brazil
- 116 Universidade Estadual de Campinas (UNICAMP), Campinas, Brazil
- 117 Université de Lyon, Université Lyon 1, CNRS/IN2P3, IPN-Lyon, Villeurbanne, France
- 118 University of Houston, Houston, Texas, United States
- 119 University of Technology and Austrian Academy of Sciences, Vienna, Austria
- 120 University of Tennessee, Knoxville, Tennessee, United States
- 121 University of Tokyo, Tokyo, Japan
- 122 University of Tsukuba, Tsukuba, Japan
- 123 Eberhard Karls Universität Tübingen, Tübingen, Germany
- 124 Variable Energy Cyclotron Centre, Kolkata, India
- 125 Vestfold University College, Tonsberg, Norway
- 126 V. Fock Institute for Physics, St. Petersburg State University, St. Petersburg, Russia
- 127 Warsaw University of Technology, Warsaw, Poland
- 128 Wayne State University, Detroit, Michigan, United States
- 129 Wigner Research Centre for Physics, Hungarian Academy of Sciences, Budapest, Hungary
- 130 Yale University, New Haven, Connecticut, United States
- 131 Yildiz Technical University, Istanbul, Turkey
- 132 Yonsei University, Seoul, South Korea
- 133 Zentrum für Technologietransfer und Telekommunikation (ZTT), Fachhochschule Worms, Worms, Germany